ELSEVIER

Journal of Structural Geology 30 (2008) 451–463

JOURNAL OF STRUCTURAL GEOLOGY

www.elsevier.com/locate/jsg

Quaternary temporal stability of a regional strike-slip and rift fault intersection

V. Mouslopoulou [a,*], A. Nicol [b], J.J. Walsh [c], D. Beetham [b], V. Stagpoole [b]

[a] School of Earth Sciences, PO Box 600, Victoria University of Wellington, Wellington, New Zealand
[b] GNS Science, PO Box 30368, Lower Hutt, New Zealand
[c] Fault Analysis Group, School of Geological Sciences, University College Dublin, Dublin 4, Ireland

Received 18 June 2007; received in revised form 10 December 2007; accepted 18 December 2007
Available online 24 December 2007

Abstract

Intersecting strike-slip and normal fault systems form either two or three plate configurations. In circumstances where they intersect to form a triple junction, internal block deformation produces a quasi-stable 3-D configuration permitting maintenance of both the regional geometry and kinematics of the intersection. This paper examines the temporal stability of such a triple junction in New Zealand over a range of timescales, from individual earthquakes to millions of years, and discusses the factors that impact its stability. Using seismic-reflection, gravity, drill-hole and outcrop data, the accumulation of vertical displacements is examined, both on individual faults and across the intersection zone between the strike-slip North Island Fault System (NIFS) and the Taupo Rift. Fault-throws and throw rates for the NIFS and Taupo Rift suggest that despite a three-fold increase in throw rates in both fault systems at about 0.3 Ma, which may have modified the orientation of the slip vectors and therefore the contemporary kinematics of the triple junction, the intersection of the two fault systems has functioned coherently for the last 0.6–1.5 Myr accumulating vertical displacements interdependently since the early stages of rifting. The apparent arrest of a large magnitude earthquake on the rift-bounding fault adjacent to the intersection, suggests that the short-term dynamic behaviour of the system is relatively complex compared to the more coherent long-term kinematics.

Keywords: Kinematic coherence; Long-term vertical displacements; Earthquake slip; North Island Fault System; Taupo Rift; New Zealand

1. Introduction

Many examples exist globally of intersecting active strike-slip and normal fault systems, including the Red Sea Rift–Dead Sea Transform, Sumatra Fault–Sunda Strait Rift, North Anatolian Fault–North Aegean Rift and numerous fracture zone–mid ocean ridges (see Mouslopoulou et al., 2007a and references therein for details). While the relative strike and abutting relations of the component fault systems may vary from one intersection to another, the orientation of the fault slip vectors must, by definition, change across the intersection. The geometries of the component faults dictate whether this change in the orientation of slip vectors requires adjustments in the slip azimuth, pitch or both. The fault geometries also impact the life expectancy and stability of the fault intersection. In circumstances where the intersecting faults form a triple junction (i.e. a three plate configuration) and result in the translation of rigid blocks, the geometry will only be stable in map view when the two arms of the strike-slip fault are in alignment or the two rift arms intersect at 90° (McKenzie and Morgan, 1969; York, 1973). Relaxing the rigid-block condition by, for example, broadening the zone of distributed off-fault deformation at block boundaries may induce quasi-stable intersections (Mouslopoulou et al., 2007a). For strike-slip and rift intersections considered to be quasi-stable, determining intersection evolution and key factors for stability is important.

* Corresponding author. Fault Analysis Group, School of Geological Sciences, University College Dublin, Dublin 4, Ireland. Tel.: +353 1 7162611; fax: +353 1 716 2607.
E-mail address: vasso@fag.ucd.ie (V. Mouslopoulou).

0191-8141/$ - see front matter © 2008 Elsevier Ltd. All rights reserved.
doi:10.1016/j.jsg.2007.12.005

In this paper we examine the Quaternary evolution and stability of the intersecting regional strike-slip North Island Fault System and the Taupo Rift in New Zealand, which form a triple junction at which the strike-slip fault terminates (Fig. 1). Landforms displaced by the NIFS over the last 30 kyr indicate that the component of dip-slip along the strike-slip faults increased northwards, towards their intersection with the Taupo Rift (Mouslopoulou et al., 2007a). These Late Quaternary displacements are transferred across the intersection and, as a consequence, strike-slip and normal fault systems are kinematically coherent (Mouslopoulou et al., 2007a). Similar coherence has been demonstrated for normal fault systems (e.g., Walsh and Watterson, 1991; Nicol et al., 2006), but the details of fault interaction have not been widely documented for synchronously intersecting strike-slip and normal fault systems. We examine the geometric and kinematic stability of this fault intersection by analyzing displacements that accumulated over a range of timescales from individual earthquakes to 1–2 million years. To determine precisely how displacements are transferred across fault intersections and to assess the stability of the current kinematics of the intersection zone (i.e. slip vector pitch and azimuth), we use seismic-reflection, gravity, drill-hole and outcrop data to chart the accumulation of vertical displacements (i.e. fault throws) on both fault systems, along individual faults and across the intersection zone (Fig. 2).

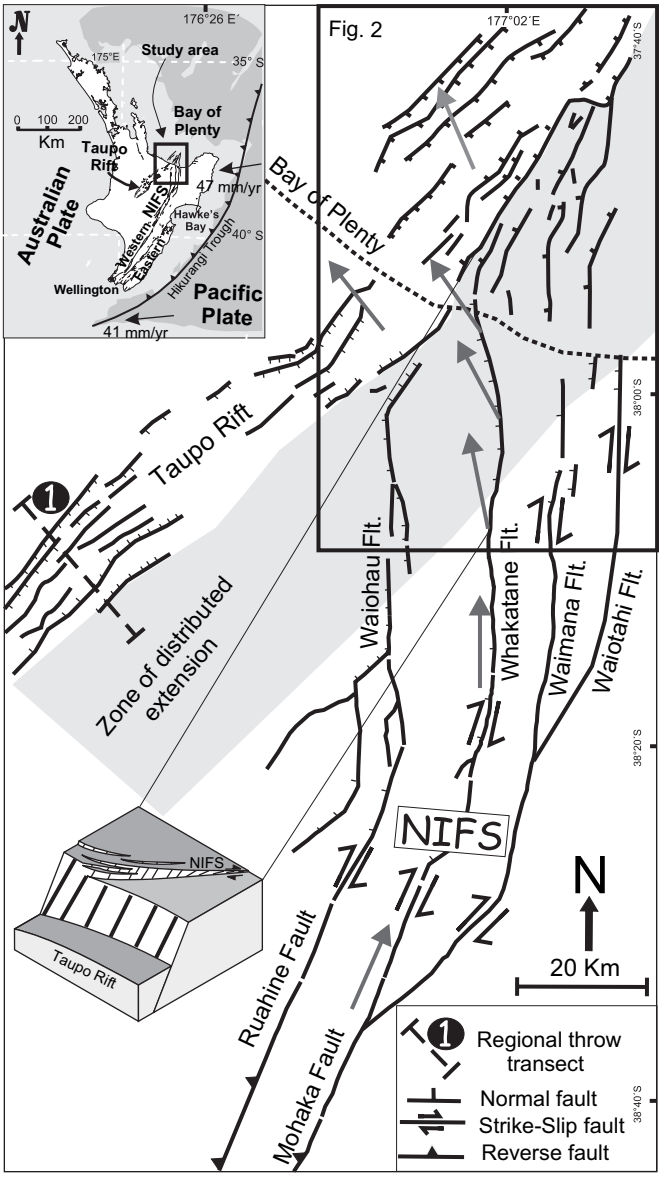

Fig. 1. Regional fault map shows the northern North Island Fault System (NIFS) intersecting obliquely, and terminating against, the Taupo Rift. Grey arrows along the two fault systems represent average net-slip azimuths (Mouslopoulou et al., 2007a). Block diagram on bottom left illustrates the steepening of the slip vectors on the NIFS with increasing proximity to the rift. Note that the block diagram is oriented in the opposite sense to the fault map. Zone of distributed extension outside the main rift is shaded grey. Thick dashed line indicates approximate location of regional throw transect-1. Inset: The North Island, New Zealand, where the Pacific Plate is being obliquely subducted beneath the Australian Plate. Relative plate motion vectors are from De Mets et al. (1994).

2. Geological setting and data

The intersecting strike-slip North Island Fault System and Taupo Rift formed in response to the westward oblique subduction of the oceanic Pacific Plate beneath the continental Australian Plate which takes place along the Hikurangi margin (Fig. 1, inset) (Ballance, 1975; Rait et al., 1991; Beavan and Haines, 2001). The North Island Fault System comprises two strands, the western and eastern (Fig. 1 inset; Beanland, 1995), however, this study focuses only on the western strand which extends further north to intersect the Taupo Rift; this strand is hereafter referred to as the 'NIFS'.

The NIFS is the longest and the highest slip-rate active fault system in the upper Australian Plate (Fig. 1, inset), strikes parallel to the Hikurangi margin (NE-SW) and dips steeply (>80°) along most of its length (Beanland, 1995; Mouslopoulou et al., 2007b). The cumulative strike-slip rate in the NIFS increases southwards, from ca. 4 mm/year in the Bay of Plenty (i.e. in the intersection zone) to ca. 10 mm/year near Wellington in the south (inset in Fig. 1), and accommodates up to 30% of the margin parallel component of the Australian–Pacific relative plate motion (Nicol and Wallace, 2007).

At its northern end, the NIFS branches into five separate splays that terminate against, and strike at ca. 45° to, the active Taupo Rift (Fig. 1). The Taupo Rift is ca. 200 km long, up to 40 km wide and comprises normal faults with typical dips of 60–70° SE and NW in the upper 2 km of crust (Rowland and Sibson, 2001; Villamor and Berryman, 2001). At the latitude of the intersection zone, extension across the rift is dominated by the Edgecumbe–White Island Fault, which is at least 50 km long and forms the eastern margin of the rift. The cumulative extension rate across the rift ranges from <4 mm/year in the south (Villamor and Berryman, 2006) to ca. 15 mm/year in the north (Davey et al., 1995; Wallace et al., 2004). Near the Bay of Plenty coast (Fig. 1), where the NIFS intersects obliquely the Taupo Rift, the rift accommodates a ca. 10 mm/year extension rate. The northward increase in extension along the Taupo Rift has been mainly attributed to differential clockwise vertical-axis rotation of

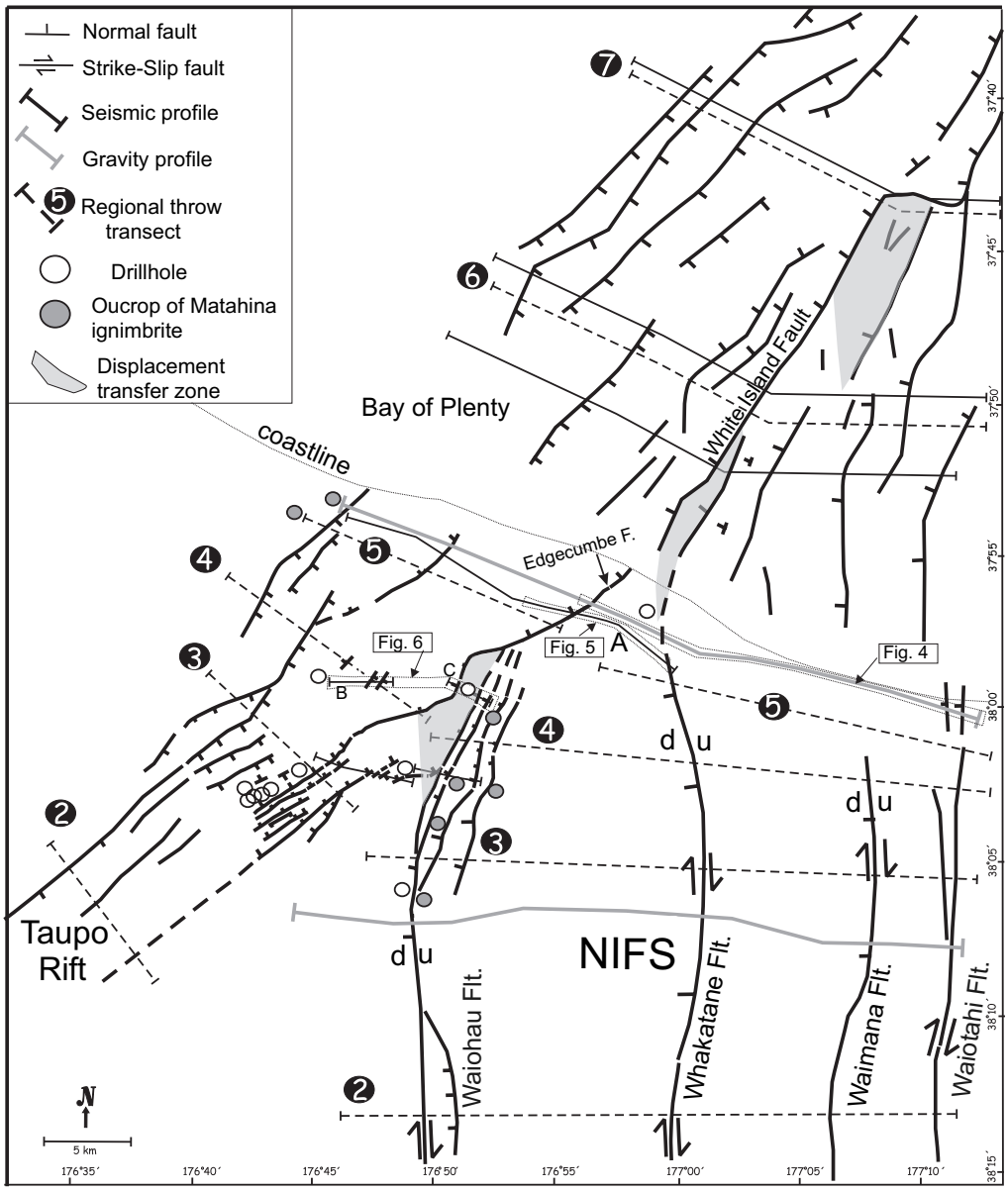

Fig. 2. Fault map showing the intersection zone between the northern NIFS and Taupo Rift. Regional throw transects (2–7) are indicated by dashed lines (see Fig. 1 for location of transect-1). Seismic-reflection profiles are from Woodward (1988), O'Connor (1988), Davey et al. (1995), Woodward-Clyde (1998), Taylor et al. (2004), Lamarche et al. (2006), Mouslopoulou (2006) and SGN Science unpublished data. The onshore multichannel seismic reflection profiles are migrated with reflectors down to two-way travel times (TWT) of 2 s (Woodward, 1988; O'Connor, 1988; Woodward-Clyde, 1998; Mouslopoulou, 2006). The bulk of the offshore seismic data consist of 3.5 kHz and migrated multi-channel seismic (MCS) reflection profiles that provide data down to 0.04 and 1.5 s, respectively (Davey et al., 1995; Lamarche et al., 2006). Regional gravity profiles are from Mouslopoulou, 2006. For more details about the gravity and seismic data (including the seismic and gravity profiles along transect 3) refer to Mouslopoulou (2006) (an electronic version of Mouslopoulou (2006) can be obtained upon request from the School of Geological Sciences at Victoria University of Wellington, New Zealand). Drillhole data are from Woodward (1988), Woodward-Clyde (1998) and Nairn and Beanland (1989), and provide additional control on the depth of basement greywacke and the Matahina ignimbrite. Offshore faults are from Davey et al. (1995), Taylor et al. (2004) and Lamarche et al. (2006). Shaded areas near fault intersections indicate zones where vertical displacement is being transferred between the component faults by bed rotations and/or sub-resolution faults (i.e. soft-linkage).

the crust across the rift (Beanland and Haines, 1998; Wallace et al., 2004; Nicol and Wallace, 2007), and may be complemented by southward propagation of the rift (Villamor and Berryman, 2006).

The Late Quaternary (ca. 30 kyr) geometries and kinematics of faults in the NIFS change conspicuously with spatial proximity to the Taupo Rift (Mouslopoulou et al., 2007b). Approximately 50–60 km south of their termination, the dips on the faults in the NIFS begin to decrease gradually, from ca. 90° to ca. 60° W, northwards near the intersection. Along the same section of the NIFS, the corresponding slip vectors on the faults steepen northward from strike-parallel (horizontal), in the south, to 60° NW, in the north, adjacent to the rift margin. These changes, which have been attributed to the superimposition of NW-SE distributed extension onto the northern section of the NIFS (Mouslopoulou et al., 2007b), generate a gradual anticlockwise rotation of the mean net-slip azimuth of the faults in the NIFS, as they approach the Taupo Rift

from the south (Fig. 1). As a consequence of these changes, at the point of fault intersection, slip vectors on the two mutually active fault systems are sub-parallel to one another and parallel to their plunging intersection line. This parallelism allows the strike-slip component of slip in the NIFS to be transferred into the rift without the margin of the rift being obviously offset and with the overall geometry of the junction being unchanged (Fig. 1) (Mouslopoulou et al., 2007b).

The intersecting fault systems displace both basement rocks of the Mesozoic Torlesse Supergroup greywacke (Mortimer, 1994) and unconformably overlying sedimentary rocks, unconsolidated sediments and volcanics that range in age from Cretaceous to Holocene (Nairn and Beanland, 1989). Torlesse greywacke basement rocks crop out extensively inland from the Bay of Plenty, but approaching the Taupo Rift along the NIFS they become progressively buried by a thick sequence ($\leq$3 km) of predominantly Quaternary marine and non-marine strata and volcanic rocks (Nairn and Beanland, 1989; Bailey and Carr, 1994). The age of strata resting directly on basement varies. On the northwestern margin of the rift, within the rift and in the hangingwall of the Waiohau Fault, K-Ar dating, geochemistry of volcanic rocks and analysis of sedimentation rates suggest that basal sedimentary strata and ignimbrite units date about 1–1.5 Ma (O'Connor, 1988; Woodward, 1988, 1989; Nairn and Beanland, 1989; Davey et al., 1995; Woodward-Clyde, 1998; Nairn, 2002; Taylor et al., 2004; Lamarche et al., 2006; Mouslopoulou, 2006). The onset of this sedimentation and volcanism was approximately coincident with the initiation of rifting at ca. 1–2 Ma (Wilson et al., 1995). On the eastern shoulder of the rift, and east of the Waiohau Fault across the NIFS, ca. 0.6 Ma marine and non-marine strata typically rest on basement (Fleming, 1955; Healy et al., 1964; Beu, 2004). These strata are overlain by a sequence of ignimbrites, tuffs and other volcanics, the most widespread of which in the study area is the Matahina ignimbrite (Bailey and Carr, 1994). Fission-track dating of zircons within the pumice indicates an age of 0.28 $\pm$ 0.03 Ma for the Matahina ignimbrite (Bailey and Carr, 1994).

Since the Matahina ignimbrite was deposited during faulting, analysis of fault displacements of the ignimbrite and the underlying top-basement unconformity provide a means of assessing the kinematics of the intersection zone of the NIFS and Taupo Rift, from the commencement of Quaternary sedimentation on basement through to the present. Gravity models, seismic-reflection profiles, drillhole data and outcrop geology (see Fig. 2 for locations and sources of data) were used to construct structure contour maps (e.g., Fig. 3) (Mouslopoulou, 2006) and to measure fault throws (i.e., the vertical component of displacement) on top-basement and top-Matahina surfaces. We take fault throws as our primary measure of fault displacement because they represent the most robust measure of dip-slip displacements from the available data (spatial data densities are insufficient to define fault heave) and because no constraints can be derived for strike-slip motions from the existing structure contour maps. Within the intersection zone, we analyse displacements along individual faults and on seven sub-parallel transects (Fig. 2) that cross the entire intersection zone (i.e. across both intersecting fault systems). For the Edgecumbe Fault, these long-term displacements are augmented by slip at the ground surface from the 1987 M6.3 Edgecumbe earthquake.

The main features of the structure of the intersection zone are highlighted by examination of the structure contour map for the top-basement (Fig. 3). The structure of the Taupo Rift is dominated by the hangingwall low of the westward-dipping Edgecumbe Fault, which gives way southwestward to a rift geometry signified by eastward dipping faults (Fig. 3). This polarity change is replaced further southward by a more symmetrical graben geometry south of Line 1 on Fig. 1, which is nevertheless dominated by a westward dipping fault (Paeroa Fault) (Villamor and Berryman, 2001; Nicol et al., 2006). Faults in the NIFS change strike particularly within ca. 10 km of the Taupo Rift. Associated displacement changes are less clear at map scale, but are reflected in the presence of larger throws and associated hangingwall lows adjacent to the northern sections of the Waiohau and Whakatane faults.

3. Vertical displacement variations of intersecting fault systems

Displacement transfer across the NIFS and Taupo Rift intersection is indicated by fault throws on the top Matahina ignimbrite (0.28 Ma) and top-basement (0.6–1.5 Ma) and by Late Quaternary (ca. 30 kyr) throw rates (Mouslopoulou et al., 2007a). In the NIFS these displacements, which range up to ca. 900 m on top-basement, are consistently down to the west and generally increase northward and westward along and across the strike of the fault system, respectively (Figs. 3, 4, 5 and 6). Fault throws in the NIFS therefore generally increase towards their intersection with the Edgecumbe–White Island Fault, which, adjacent to the intersection zone, accommodates up to 2500 m displacement and ca. 50–60% of the total throw across the rift. Given the kinematic importance of the Edgecumbe–White Island Fault, we examine its throws and throw rates where it intersects the Waiohau and Whakatane Faults (Section 3.1). These displacements are combined with those from the remainder of the rift and from the NIFS to determine the long-term displacement transfer across the entire intersection zone (Section 3.2).

3.1. Intersection of individual faults

The Waiohau Fault (NIFS) intersects and terminates against the rift-bounding Edgecumbe Fault ca. 8 km south of the Bay of Plenty coast (Figs. 1 and 2). Within ca. 10 km of this termination, the Waiohau Fault swings in strike from N-S to NNE-SSW to become sub-parallel to the strike of the Edgecumbe Fault and bifurcates into at least four sub-parallel splays (Fig. 2). The shapes of the throw profiles for the top Matahina and top-basement horizons are comparable on the Edgecumbe and Waiohau Faults across their mutual intersection (Fig. 7a and b); Waiohau Fault throws are the aggregate of its component splays. For both horizons, throws on the Waiohau Fault

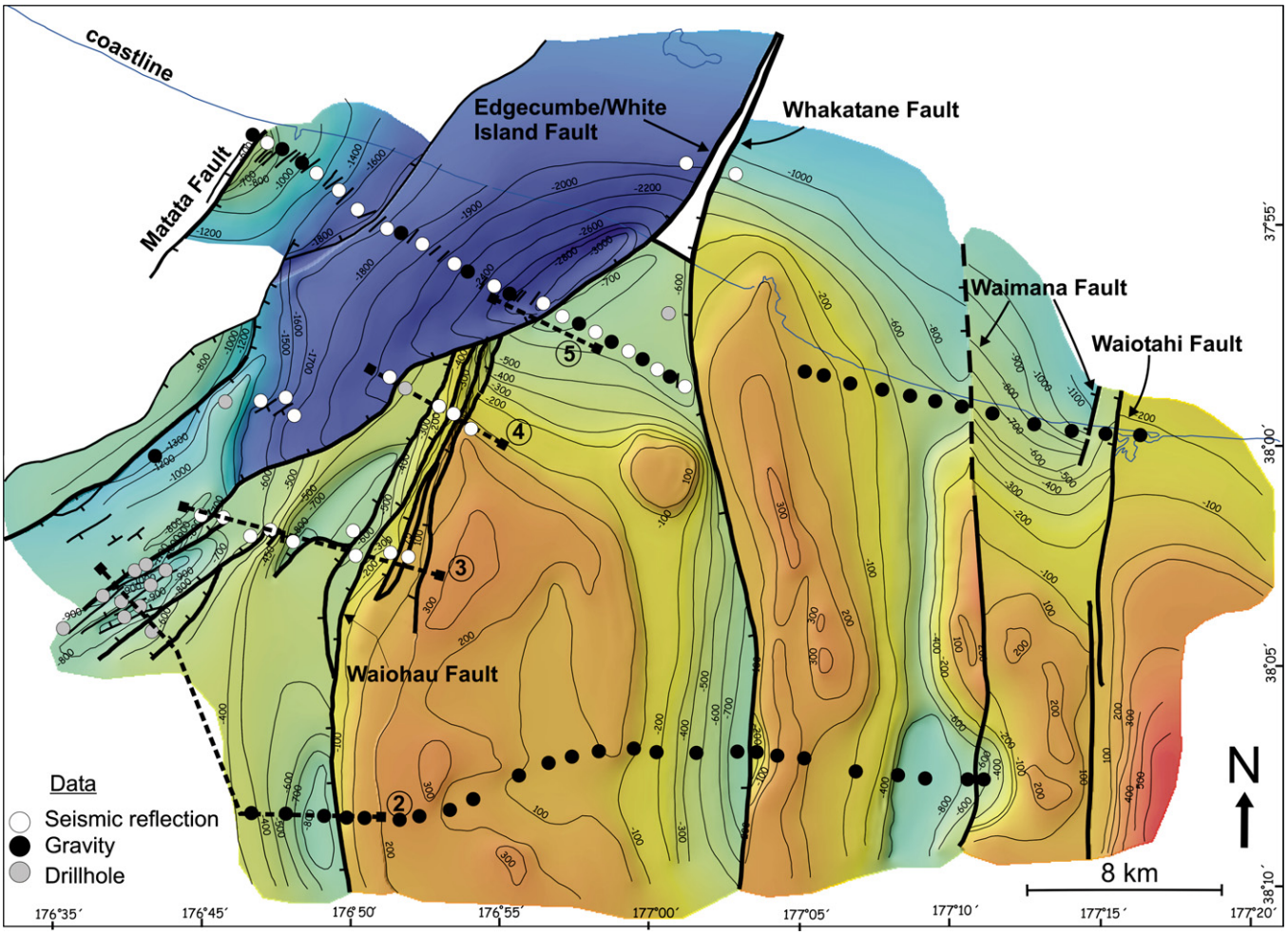

Fig. 3. Structure contour map for the top of greywacke basement in the region where the NIFS and Taupo Rift intersect. Contours are in metres above (positive) or below (negative) sea level. Data are from seismic-reflection and gravity profiles, drilling and outcrop geology (contours above zero are primarily controlled by outcrop of basement). Offshore contours are estimated from offshore residual gravity anomalies (Stagpoole and Bibby, 1999). Locations of data used to construct the contours are shown. Locations of transects used to derive throws across the Waiohau/Edgecumbe fault intersection are indicated and numbered (in order to cross-reference the numbers see Figs. 2 and 7). Warm and cold colours indicate high and low altitudes, respectively. The coastline is indicated.

increase to the northeast between 12 km and 7 km south of the intersection and then decrease gradually northwards towards the intersection. By contrast, throws on the Edgecumbe Fault decrease towards the southwest, between distances of 3 km to the north and 7 km to the south of the intersection. A significant component (~20–40%) of this southwest decrease in throw on the Edgecumbe Fault takes place across its intersection with the Waiohau Fault. On the top-basement horizon, for example, up to 600 of the ca. 2000 m decrease in throw on the Edgecumbe Fault occurs across its intersection with the Waiohau Fault. The complementary changes in vertical displacements of the Edgecumbe and Waiohau Faults are consistent with the view that displacement was transferred between the two faults (Fig. 7a). Much of this transfer is achieved via hard linkage of the faults, however, changes in their displacements up to 7 km southwest of the intersection, in particular the decrease in throw on the Waiohau Fault, suggest that displacement has also been transferred by down-to-the-west horizon rotations and/or subresolution faults, and therefore soft-linkage (Walsh and Watterson, 1991), within a rock volume which, in map view, has approximate dimensions of ca. 3 × 7 km (see shaded area on Fig. 2). This area of displacement transfer is adjacent to, and immediately west of, the splays at the northern end of the Waiohau Fault where it strikes sub-parallel to the rift. Similarities in the shapes of the throw profiles for each horizon suggest that displacement transfer between these faults via both hard and soft linkage occurred throughout fault growth, with fault intersection and interaction commencing at 0.6–1.5 Ma, perhaps coinciding with the onset of rifting.

Transfer of throw between the Waiohau and Edgecumbe faults only accounts for about half of the decrease in throw to the southwest on the Edgecumbe Fault (Fig. 7a and b). This discrepancy in displacements arises because throw on the Edgecumbe Fault is transferred southward to the Waiohau Fault and to eastward dipping faults on the west margin of the rift. Displacements transferred onto the western margin of the rift are indicated by shaded areas on Fig. 7a and b. On the top-basement horizon, for example, the southward decrease in throw on the Edgecumbe Fault accompanies an increase in

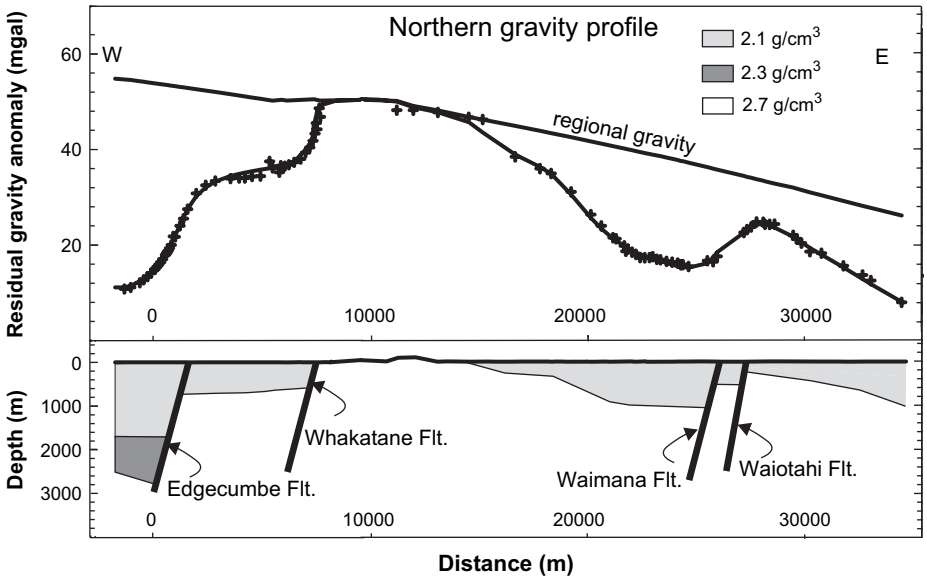

Fig. 4. Two-dimensional residual gravity profile for the northern regional sample line. Densities used for modelling range from 2.1 to 2.7 g/cm^3 (see description of the modelling in Mouslopoulou, 2006). Data show the westward increase in throw on the faults in the NIFS as the intersection with the Taupo Rift is approached. See Fig. 2 for location of the northern gravity profile.

throw from ca. 700 to 1200 m on the faults of the western margin of the rift (Fig. 7a). This displacement transfer is associated with a change in the polarity of the rift, which is dominated by the west-dipping Edgecumbe Fault in the north near the coast and by east-dipping faults along the western margin of the rift in the south (i.e. 15 km south of the coast) (Fig. 3). The aggregate (total) throw on the top-basement and top-Matahina surfaces for the rift and the Waiohau Fault across the intersection of the two fault systems between transects 4–5 (i.e. adjacent to the intersection), is approximately constant (Figs. 2 and 7). The coherence of throw variations between the Waiohau Fault, Edgecumbe Fault and faults along the western margin of the rift suggests that all faults are kinematically interdependent.

The kinematic coherence between individual faults in the NIFS and Taupo Rift is further demonstrated for the offshore intersection of the Whakatane–White Island faults (Figs. 2 and 8). The latter fault is the offshore lateral equivalent of the Edgecumbe Fault. Late Quaternary throw rates on the Edgecumbe–White Island Fault are less immediately south of its intersection with the Whakatane Fault than north (Fig. 8). The 1.5–2.5 mm/year decrease in rate on the Edgecumbe–White Island Fault approaching the intersection, from the south, is approximately equal to the 2.3 ± 0.9 mm/year throw rate on the Whakatane Fault 5 km south of the intersection. This decrease indicates that a fraction of the total strain in the rift is locally accommodated by, and transferred to, the Whakatane Fault (Fig. 8). The complementary nature of throw-rate variations across this fault intersection, reflects the efficient displacement transfer where both faults are subparallel and close to each other. As is the case across the intersection of the Edgecumbe and Waiohau Faults, the aggregate throw on the White Island and Whakatane faults is maintained across their intersection. In a similar manner to the Waiohau Fault, throw rates on the Whakatane Fault increase northwards to a maximum 5 km from its intersection with the White Island Fault and then decrease to 20–40% of the maximum at the intersection. Again, these data support the notion that displacement transfer has been achieved by hard and soft linkage, with the latter being particularly important where the intersecting fault (i.e. Whakatane Fault) becomes sub-parallel to the rift (and the Edgecumbe–White Island Fault).

The consistency in displacement transfer between different fault intersections, and for a range of time periods, attests to the stability of fault intersections and their associated interaction. It also suggests that displacement transfer via hard and soft linkage is synchronous and that fault interaction began during the early stages of rifting (i.e. 0.6–1.5 Ma). The uniformity of fault kinematics at these intersections leads to the inference that similar displacement transfer is likely to occur where the White Island Fault intersects the Waimana and Waiotahi faults of the NIFS.

3.2. Entire intersection zone

Kinematic coherence between individual intersecting faults is reflected in the throw variations observed at a more regional scale across the entire intersection zone. To examine regional fault kinematics we estimate the total throw on the top-basement surface across both intersecting fault systems on seven regional transects (see Figs. 1 and 2 for locations of transects). The number of faults in the NIFS that are included within each transect decreases to the north as progressively more of these faults terminate against the Taupo Rift (Fig. 2). Collectively the regional profiles suggest that the total throw accrued on the top-basement surface across the intersection of the two fault systems increases gradually northwards by about 1–1.5 km over a distance of 60 km (Fig. 9). This increase in

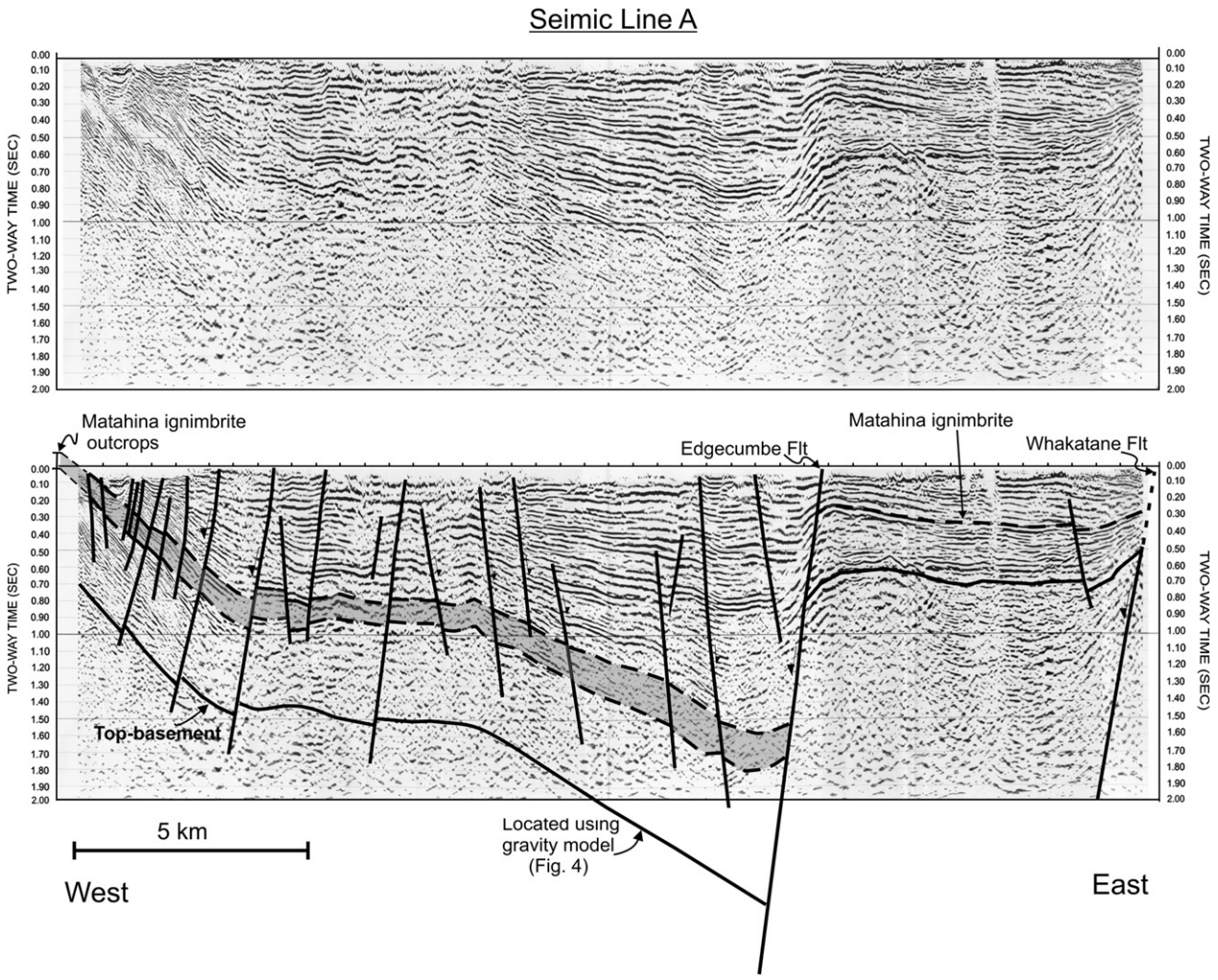

Fig. 5. The onshore seismic-reflection profile A across the Rangitaiki Plains (see Fig. 2 for location) with and without interpreted horizons, is illustrated. The position of the top of the greywacke basement (solid line) west of Edgecumbe Fault is estimated from the northern gravity profile in Fig. 4. The location of the Matahina ignimbrite (black dash-lined shaded polygon) is estimated by projecting outcropping Matahina ignimbrite located ca. 500 m beyond the western end of the seismic line (see Fig. 2 for location of outcrop) onto the western margin of the Taupo Rift and by tracing the associated reflector eastwards onto the Edgecumbe Fault. The vertical dimension of the shaded polygon indicates the uncertainty of the vertical location of the top-Matahina ignimbrite surface. A drillhole on the hangingwall of the Whakatane Fault constrains the depth to top-basement. Depth is in two-way-traveltime (TWT) seconds and the vertical exaggeration ca. 5.

cumulative (total) throw is replicated by a general northward increase of throw on the faults in the NIFS and is consistent with a northward increase of the contemporary extension along the rift determined from GPS modelling (Wallace et al., 2004).

The region over which extension is accommodated widens where the NIFS intersects the rift. To the south and north of the NIFS in Fig. 9, the total throw on both fault systems is entirely accommodated by the rift. In the intervening region where the two fault systems intersect (i.e. −40 to 40 km on Fig. 9), typically 20–40% of the total throw is distributed outside the rift and accommodated by the NIFS. As the profile of total throw is less variable than the individual profiles for the rift and the NIFS, the throw data support the suggestion that the large faults incorporated into Fig. 9 from the NIFS and the rift are kinematically interdependent, even though they are separated by up to 50 km (i.e. perpendicular to strike) and do not all intersect. The gradual and systematic manner in which this regional-scale fault interaction accommodates displacement transfer by both hard- and soft-linkage is reflected in the fact that fault intersections are not easily identifiable from the total throw profile in Fig. 9. Indeed, within the region where the two fault systems intersect (i.e. −40 to 40 km on Fig. 9), distinguishing faults in the NIFS and the rift proper becomes more problematic as the zone across which extension is accommodated broadens from 15–20 km wide to ca. 60 km. The associated widening of the region of extension results from the gradual northward transformation of the strike-slip motions of the NIFS into dip-slip motion along the rift (Mouslopoulou et al., 2007b).

4. Earthquake slip at fault intersections

The faults of the NIFS and the Taupo rift are currently active and historical data suggest that slip at the surface mainly

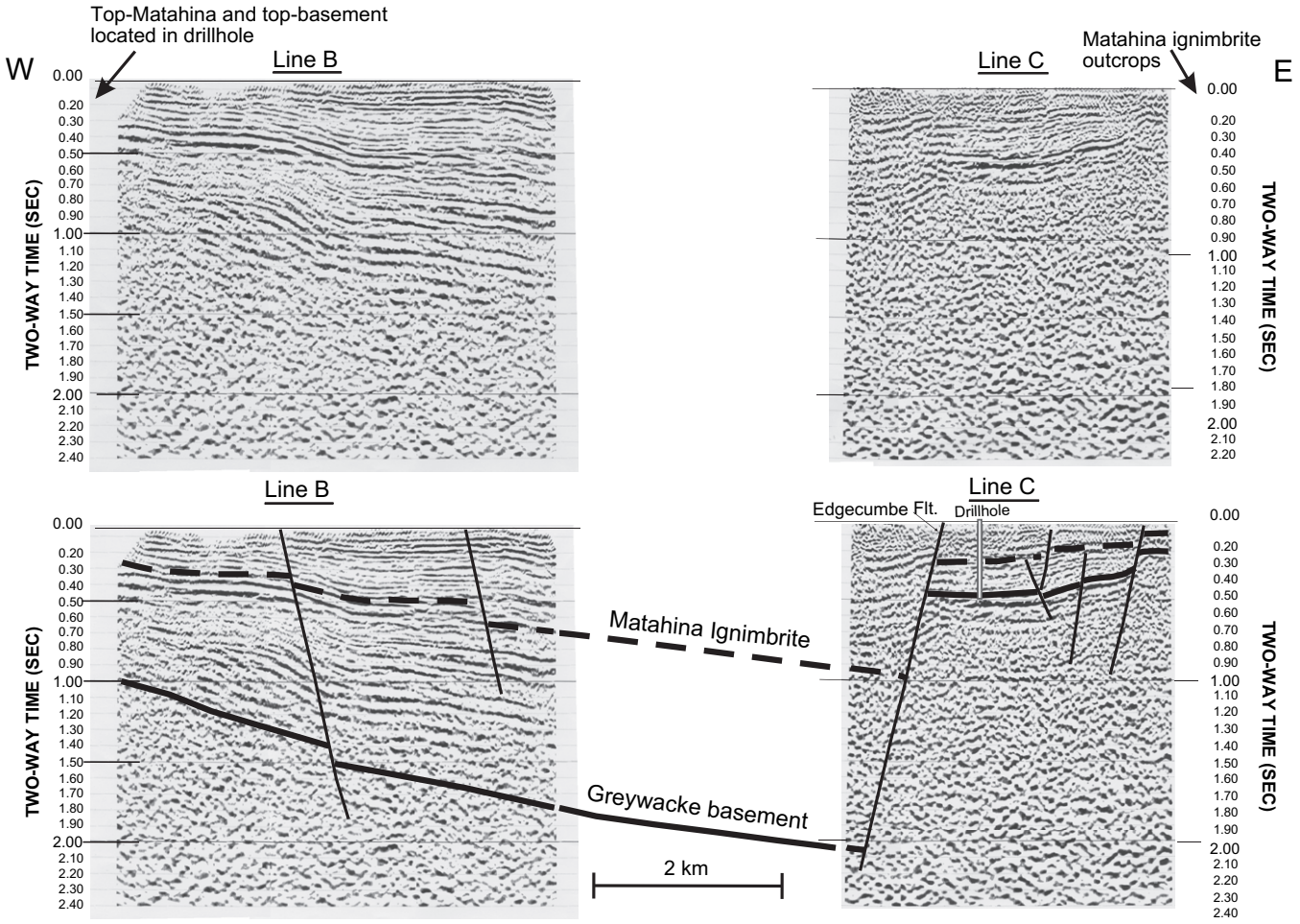

Fig. 6. Uninterpreted/interpreted seismic reflection profiles B and C across the eastern half of the Taupo Rift and the Waiohau Fault (see Fig. 2 for location). Two-way traveltime to top Matahina ignimbrite and to top-basement on profiles B and C are constrained by drillhole data (see Fig. 2 for location of the drillholes). Vertical exaggeration ca. × 5.

accrues during large-magnitude earthquakes (because evidence for creeping faults at the ground surface is absent in New Zealand). In this section we examine how these earthquakes combine to produce vertical displacement changes and kinematic coherence of the intersecting fault systems on time scales of thousands to millions of years.

The largest historical earthquake within the Taupo Rift (Mw 6.3, 1987 Edgecumbe earthquake, Beanland et al., 1989) ruptured the Edgecumbe Fault close to its intersection with the Waiohau Fault (Figs. 1 and 2). Geological and seismological evidence indicate that fault rupture initiated in the north and propagated southwards for a strike distance of ca. 14 km (Anderson and Webb, 1989; Beanland et al., 1989) (Fig. 10). The northern end of the rupture coincides approximately with the intersection zone of the Waiohau and Edgecumbe faults (Fig. 10). The slip profile is slightly asymmetric with modestly greater slip gradients developed adjacent to the intersection zone as compared to the more gradual slip decrease towards the southern tip of the Edgecumbe Fault. The proximity of the northern end of the 1987 rupture to the Edgecumbe–Waiohau fault intersection and the asymmetry of this slip profile indicate that rupture initiation close to the fault intersection was possibly controlled by changes in the geometry and local stresses along the Edgecumbe Fault, proximal to its intersection with the Waiohau Fault.

The southward decrease in the throw distribution during the 1987 Edgecumbe earthquake is comparable, to a first order, with that of the decline in throws on the top-basement surface (Fig. 10). The similarity in the normalised displacement profiles for the 1987 earthquake and for the top-basement along the southern ca. 10 km of the fault (i.e. between 10 and 20 km on Fig. 10) is consistent with the view that many large magnitude earthquakes on the southern segment of the Edgecumbe Fault carried slip profiles comparable to the 1987 Edgecumbe earthquake. Replication of the long-term displacement distribution on the Edgecumbe Fault demands, however, that any slip deficits immediately south of the intersection, must be removed either by off-fault deformation (e.g. bed rotations) and/or by large magnitude events which rupture across the intersection. While we cannot discount the possibility that some large magnitude earthquakes on the Edgecumbe Fault rupture through its intersection with the Waiohau fault, there are indications that the intersection plays a profound role in the accumulation of slip

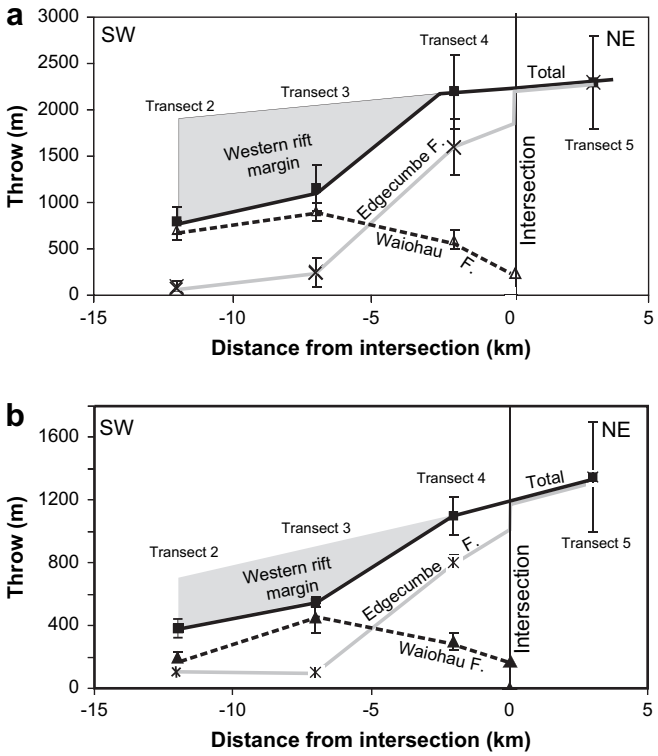

Fig. 7. Plot showing the throw on the Waiohau and Edgecumbe faults at four transects across their intersection for (a) the top-basement surface (0–1.5 Ma) and (b) the top Matahina Ignimbrite (0–0.28 Ma); refer to Fig. 2 for locations of transects. Note that in transects 3 and 4, the throw measured across the Waiohau Fault is the aggregated throw across all four strands. Furthermore, as pre-0.6 Ma strata are eroded from the footwall of the Waiohau Fault, top-basement (0–1.5 Ma) throws on this fault are a minimum estimate. The aggregated (total) throw across the Waiohau and Edgecumbe faults at each transect is indicated by the black solid line. The southward deficit of the total throw across the intersection (grey polygon) is accounted for by displacement transfer onto faults that define the western margin of the rift. For simplification, the intersection is presented as a line although it comprises a zone.

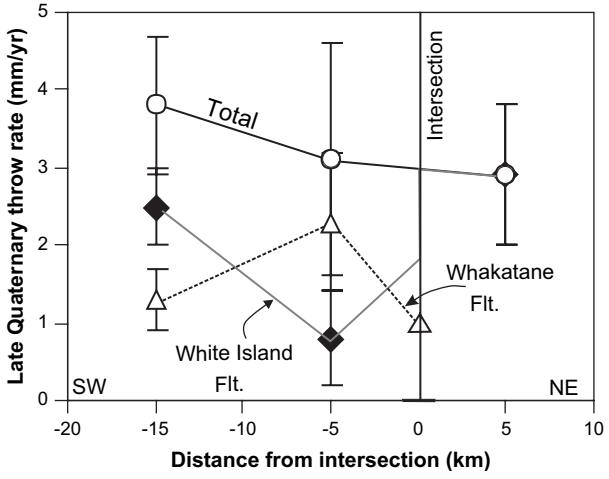

Fig. 8. Late Quaternary (0–18 kyr) throw rates for the Whakatane and White Island (Edgecumbe) faults across their intersection plotted against distance from their intersection. The total throw is also indicated. Onshore throw rate data are from Beanland et al. (1989) and Mouslopoulou (2006) whereas offshore data are from Lamarche et al. (2006).

on earthquake time-scales. For example, the notion that individual earthquakes generally do not rupture through the intersection zone of the Edgecumbe and Waiohau faults (i.e. do not rupture both faults) is consistent with their recurrence intervals. Recurrence intervals on the Waiohau Fault (3.6 ± 1.2 kyr) during the last 13 kyr are, for example, a factor of 4 to 8 times longer than those on the Edgecumbe Fault south of the intersection zone (ca. 0.6 kyr) (Mouslopoulou, 2006). As a consequence, the timing of slip events on the Edgecumbe and Waiohau Faults must, in most cases, be different. Based on their Late Quaternary (0–13 kyr) recurrence intervals, it is however possible that slip events on the Waiohau Fault could either trigger, or be triggered by, up to 25% of the ruptures on the Edgecumbe Fault. Whilst it is possible, therefore, that ruptures of the Edgecumbe Fault could produce slip on the Waiohau Fault, this was not the case in 1987. The available evidence suggests therefore that the interdependent long-term displacements on the Edgecumbe and Waiohau Faults have mainly arisen from earthquakes that did not rupture through their fault intersection. These earthquakes may locally increase or decrease the static stresses (e.g. Robinson, 2004) which, in turn, enhance or depress, respectively, the probability of future earthquakes on the adjacent faults within the intersection zone.

In conclusion, the accumulation of displacement across an active strike-slip and normal fault intersection when averaged over thousands to millions of years is uniform, but this uniformity has most likely been produced by earthquakes that ruptured the component faults of the intersection zone during different slip events. Thus, although earthquake slip may sometimes be arrested or accentuated at, or close to, such intersections, displacements accumulated during geological timescales do not reflect this earthquake slip sensitivity.

5. Kinematic history of intersection zone

Comparison of average throw rates for different age horizons provides information on temporal changes of fault kinematics. Average throw rates on the Edgecumbe Fault in the rift and the Waiohau Fault in the NIFS were greater post 280 kyr (i.e. post-Matahina ignimbrite) than prior to this time (Fig. 11). An increase in throw rates during the Late Quaternary is consistent with Holocene rates on the Whakatane, Waimana and Waiotahi Faults (ca. 2.3 mm/year, 1.1 mm/year, 0.7 mm/year, respectively) being greater than the time-averaged rates estimated from the top-basement unconformity (ca. 1.1 mm/year, 0.8 mm/year, 0.5 mm/year, respectively) (Mouslopoulou, 2006). The observed post 280 kyr increases in fault throw rates are generally about a factor of 2–3 for individual faults (i.e., Edgecumbe and Waiohau faults), and for different regional transects across the active Taupo Rift (Fig. 11). This increase in fault throw rates appears to be contemporaneous with a previously interpreted change in the structure of the rift, characterised by an eastward migration and localisation of the locus of NW-SE extension (Davey et al., 1995). Therefore the migration of extension may be partially responsible

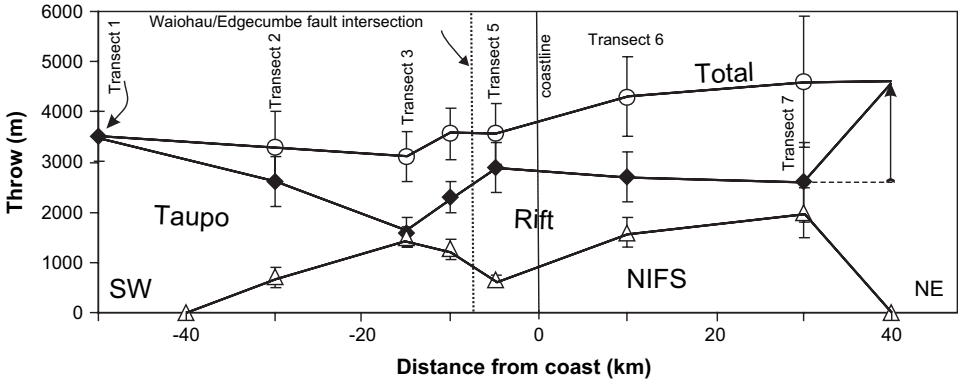

Fig. 9. Throw accrued on the top-basement across the Taupo Rift (black rhomb), the NIFS (open triangle) and their intersection (open circle) plotted against distance from the Bay of Plenty coastline. For location of the regional throw transects refer to Figs. 1 and 2. North of transect 7, on the right hand side of the graph at ca. 40 km offshore, where the NIFS terminates against the rift, the total throw is accommodated entirely by the faults in the Taupo Rift. The black arrow at ca. 40 km offshore indicates the ca. 2 km increase in the throw across the rift required to maintain a constant total throw north of transect 7.

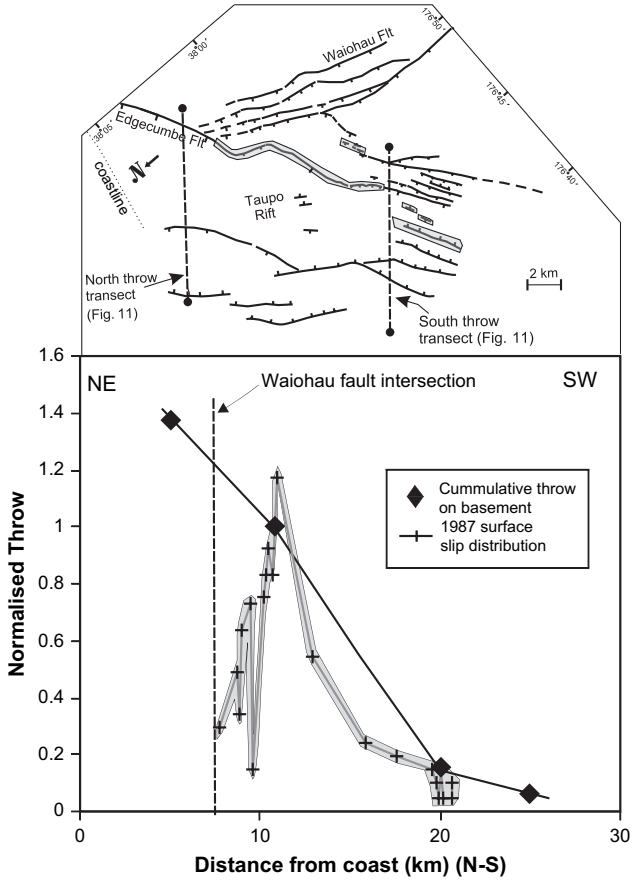

Fig. 10. Normalised vertical displacements on top-basement surface for the Edgecumbe Fault compared with the surface throw distribution of the 1987 Edgecumbe earthquake. Throws in each dataset are normalised to the slip at ca. 11 km south of the coast. The two datasets are plotted against southward strike distance along the Edgecumbe Fault, from the Bay of Plenty coastline. Inset fault map shows the intersection zone with the grey polygons indicating the surface slip distribution of the 1987 Edgecumbe earthquake (Beanland et al., 1989; Begg and Mouslopoulou, 2007). North and south throw transects across the rift (see Fig. 11) are indicated with dashed lines.

for the increase in the throw rates on the faults in the NIFS in the last 280 kyr (Mouslopoulou, 2006; this study). Synchronous increases in throw rates on both fault systems also reinforce the notion that the junction of the two fault systems is kinematically coherent.

The precise timing of the onset of accelerated extension across the active rift and NIFS is difficult to define, but certainly pre-dates 0.28 Ma and deposition of the Matahina ignimbrite and post-dates the youngest deposits above the top-basement unconformity (i.e. Whakatane Fault), which is ca. 0.6 Ma. Davey et al. (1995) recognise fault growth and related eastward migration of extension within the active offshore portion of the rift during the Late Quaternary. Using the seismic interpretation from Davey et al. (1995) and the constant sedimentation rates inferred by Taylor et al. (2004), the onset of accelerated extension is estimated to have

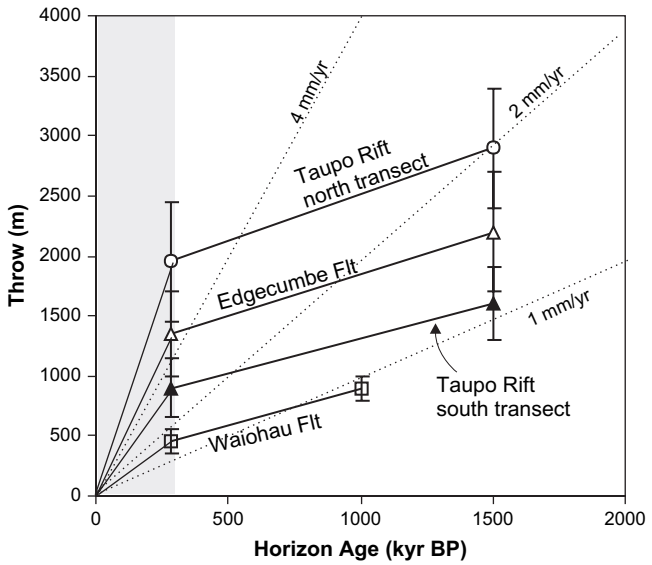

Fig. 11. Plot illustrating the accumulation of throw on increasingly older horizons for the Edgecumbe (open triangles) and Waiohau (squares) faults. The temporal variations of the aggregated, across the entire rift, throw on the north (circles) and south (black triangles) transects are indicated. The shaded region indicates minimum time period during which faults have accelerated throw rates. Throw rate contours are shown.

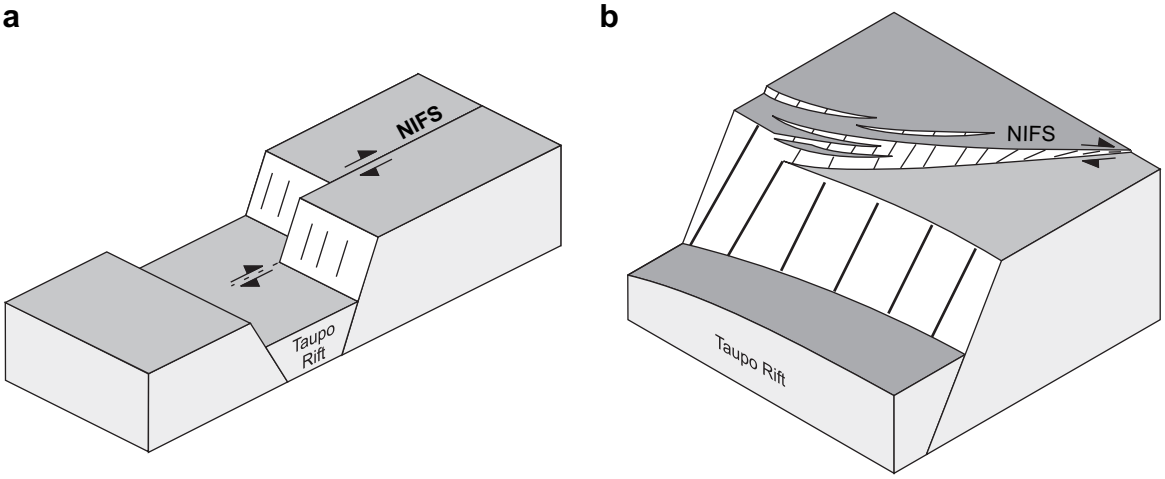

Fig. 12. Schematic block diagrams illustrate possible kinematic and geometric relationships between the NIFS and the Taupo Rift prior to ca. 0.3 Ma: (a) strike-slip rates comparable to today's rates with strike-parallel slip vectors in the NIFS offsetting the southwest rift margin, (b) strike-slip and dip-slip rates comparable to one another with displacements transferred between fault systems through sub-parallel slip vectors (black lines on fault planes indicate slip vectors).

occurred at ca. 0.3 Ma. Wilson et al. (1995) also identify 0.34 Ma as a critical time heralding a change from 'old Taupo Volcanic Zone' volcanism to 'young Taupo Volcanic Zone' volcanism, a transition that coincides with the eruption of large volumes of rhyolites in the central part of the rift. Villamor and Berryman (2006) suggest that the temporal activity of faults may also change in a similar manner, with extension preferentially concentrating at that time into a zone on the eastern side of, and about 70% of the width of, the pre-existing rift. They also conclude that faulting in the southern Taupo Rift may have commenced at this time, following its rapid southward propagation. Collectively the available data (Davey et al., 1995; Villamor and Berryman, 2006; this study) indicate a change in the geometry and kinematics of the Taupo Rift along its entire length, at a time which approximates the onset of an episode of major rhyolitic eruptions ca. 0.34 kyr ago (Wilson et al., 1995), but whether changes in the tectonics triggered the eruptions or vice versa remains a point of debate.

Late Quaternary (ca. 30 kyr BP) slip vectors in the NIFS within the intersection zone (see shaded zone in Fig. 1) have approximately equal amounts of dip-slip and strike-slip and are sub-parallel with the slip vectors in the rift (Mouslopoulou et al., 2007a) (Fig. 12b). Acceleration and eastward migration of the active rifting in the last 0.3 Ma was associated with an increase in the rates of dip-slip in the NIFS. The rates of strike-slip may, however, have remained approximately uniform since 1 Ma. This inference is based on the cumulative 5–8 km apparent strike-slip displacement of basement terranes near Wellington (Begg and Mazengarb, 1996) and the ca. 1 Ma estimate for the onset of strike-slip faulting (Kelsey et al., 1995). The long-term 5–12 mm/year strike-slip rates on the Wellington Fault in the NIFS are of a similar order to the ca. 7 mm/year Holocene rates (Van Dissen and Berryman, 1996). These data suggest that the present strike-slip rates in the NIFS possibly predate 0.3 Ma although a change in rates equivalent to that of the faults in the rift cannot be discounted. Therefore, if rates of strike-slip in the northern NIFS prior to 0.3 Ma were indeed comparable to today's rates (i.e. ca. 4 mm/year), then the pitch of slip vectors on faults in the NIFS would have been about half the Late Quaternary values. The relatively low slip-vector pitch at the termination of the faults in the NIFS prior to 0.3 Ma may either require that the southeastern margin of the rift, near Bay of Plenty, was displaced by small (<2 km) sub-resolution right-lateral strike-slip (Fig. 12a) and/or that the transfer of strike-slip to dip-slip was achieved by strike changes of faults in the NIFS close to the intersection with associated ductile deformation. If future studies support a model in which both the Taupo Rift and the NIFS are characterised by equivalent increase in rates at ca. 300 kyr, the present configuration of the junction may have been stable since its inception.

Whatever the mechanism of displacement transfer, the kinematic coherence across each strike-slip and normal fault intersection applied for the duration of faulting.

6. Conclusions

The Quaternary stability of a regional strike-slip and normal fault intersection in New Zealand is examined. Seismic-reflection, gravity, drill-hole and outcrop data were used to chart accumulation of vertical displacements proximal to the intersection of the strike-slip NIFS and the Taupo Rift over timescales of individual earthquakes to millions of years. In the vicinity of the intersection, the two fault systems have operated as a kinematically coherent fault array since at least 0.6–1.5 Ma accumulating displacements interdependently since the early stages of rifting. This uniformity in displacement accumulation during hundred to million year long timescales is interpreted to result from earthquakes that often terminated at fault intersections. Vertical displacement rates in the active part of the rift and the NIFS increased by up to a factor of 3 during the last 0.3 Myr. While this increase in rates did not impact on the kinematic coherence of the fault

intersection, it may have modified the orientation (pitch and azimuth) of the slip vectors on the component faults.

Acknowledgements

This work is the result of a PhD study undertaken at Victoria University of Wellington, New Zealand, funded by the Earthquake Commission of New Zealand and supported by the Foundation of Research, Science & Technology of New Zealand and GNS-Science (Enterprise Scholarship). We are grateful to Derek Woodward for assistance in the process of the gravity data and to Dave Heron for 'building' the Digital Elevation Model for the structural contour map in Fig. 3. J. Rowland, H. Koyi and W. Dunne (editor) are thanked for constructive reviews. Our Maori family of Tuhoe is thanked for its gentle Wairua.

References

Anderson, H., Webb, T., 1989. The rupture process of the Edgecumbe earthquake, New Zealand. New Zealand Journal of Geology and Geophysics 32, 43–53.

Bailey, R.A., Carr, R.G., 1994. Physical geology and eruptive history of the Matahina Ignimbrite, Taupo Volcanic Zone, North Island, New Zealand. New Zealand Journal of Geology and Geophysics 36, 319–344.

Ballance, P.F., 1975. Evolution of the India-Pacific plate boundary in North Island, New Zealand. Bulletin of the Australian Society of Exploration Geophysicists 6 (2/3), 58–59.

Beanland, S., 1995. The North Island Dextral Fault Belt, Hikurangi Subduction margin, New Zealand. PhD thesis, Victoria University of Wellington, New Zealand.

Beanland, S., Haines, J., 1998. The kinematics of active deformation in the North Island, New Zealand, determined from geological strain rates. New Zealand Journal of Geology and Geophysics 41, 311–323.

Beanland, S., Berryman, K.R., Blick, G.H., 1989. Geological investigations of the 1987 Edgecumbe earthquake. New Zealand Journal of Geology and Geophysics 32, 73–91.

Beavan, R.J., Haines, J., 2001. Contemporary horizontal velocity and strain rate fields of the Pacific–Australian plate boundary zone through New Zealand. Journal of Geophysical Research 106 (B1), 741–770.

Begg, J.G., Mazengarb, C., 1996. Geology of the Wellington area, scale 1:50 000. Institute of Geological & Nuclear Sciences, Lower Hutt, New Zealand, Geological Map 22. 1 sheet + 128 pp.

Begg, J.G., Mouslopoulou, V., 2007. Rangitaiki Plains: The Veil is Lifted. New LiDAR Data from Bay of Plenty. Geological Society of New Zealand Miscellaneous Publications 123A, New Zealand, ISBN 0-908678-08-8.

Beu, A.G., 2004. Marine mollusca of oxygen isotope stages of the last 2 million years in New Zealand. Part 1: Revised generic positions and recognition of warm-water and cool-water migrants. Journal of the Royal Society of New Zealand 32 (2), 111–265.

Davey, F.J., Henrys, S., Lodolo, E., 1995. Asymmetric rifting in a continental back-arc environment, North Island, New Zealand. Journal of Volcanology and Geothermal Research 68, 209–238.

De Mets, C.R., Gordon, R.G., Argus, D., Stein, S., 1994. Effect of recent revisions to the geomagnetic reversal time scale on estimates of current plate motions. Geophysical Research Letters 21, 2191–2194.

Fleming, C.A., 1955. Castlecliffian fossils from Ohope Beach, Whakatane (N69). New Zealand Journal of Science and Technology Section B36, 511–522.

Healy, J., Schofield, J.C., Thompson, B.N., 1964. Geological Map of New Zealand. 1:250,000, Sheet 5, Rotorua, first ed. Department of Scientific and Industrial Research, Wellington, New Zealand.

Kelsey, H.M., Cashman, S.M., Beanland, S., Berryman, K.R., 1995. Structural evolution along the inner forearc of the obliquely convergent Hikurangi margin, New Zealand. Tectonics 14, 1–18.

Lamarche, G., Barnes, P.M., Bull, J.M., 2006. Faulting and extension rate over the last 20,000 years in the offshore Whakatane Graben, New Zealand continental shelf. Tectonics 25, TC4005, doi:10.1029/2005TC001886.

McKenzie, D.P., Morgan, W.J., 1969. Evolution of triple junctions. Nature 224 (5215), 125–133.

Mortimer, N., 1994. Origin of the Torlesse Terrane and coeval rocks, North Island, New Zealand. International Geology Review 36, 891–910.

Mouslopoulou, V., 2006. Quaternary geometry, kinematics and paleoearthquake history at the northern termination of the strike-slip North Island Fault System, New Zealand. PhD thesis. Victoria University of Wellington, New Zealand.

Mouslopoulou, V., Nicol, A., Little, T.A., Walsh, J.J., 2007a. Displacement transfer between intersecting strike-slip and extensional fault systems. Journal of Structural Geology 29, 100–116.

Mouslopoulou, V., Nicol, A., Little, T.A., Walsh, J.J., 2007b. Terminations of large strike-slip faults: an alternative model from New Zealand. In: Cunningham, W.D., Mann, P. (Eds.), Tectonics of Strike-Slip Restraining and Releasing Bends. Geological Society of London, Special Publications, 290, pp. 387–415.

Nairn, I.A., 2002. Geology of the Okataina Volcanic Center, scale 1:50 000. Institute of Geological & Nuclear Sciences, Lower Hutt, New Zealand.

Nairn, I.A., Beanland, S., 1989. Geological setting of the 1987 Edgecumbe earthquake, New Zealand. New Zealand Journal of Geology and Geophysics 32 (1), 1–13.

Nicol, A., Wallace, L., 2007. Temporal stability of deformation rates: comparison of geological and geodetic observations, Hikurangi Margin, New Zealand. Earth and Planetary Science Letters 258 (3–4), 397–413.

Nicol, A., Walsh, J.J., Berryman, K., Villamor, P., 2006. Interdependence of fault displacement rates and paleoearthquakes in an active rift. Geology 34, 865–868.

O'Connor, R.M., 1988. Seismic reflection investigations near the Matahina Dam. DSIR Contract Report, No. 84.

Rait, G., Chanier, F., Waters, D.W., 1991. Landward- and seaward-directed thrusting accompanying the onset of subduction beneath New Zealand. Geology 19, 230–233.

Robinson, R., 2004. Potential earthquake triggering in a complex fault network: the Northern South Island, New Zealand. Geophysical Journal International 159, 734–748.

Rowland, J.V., Sibson, R.H., 2001. Extensional fault kinematics within the Taupo Volcanic Zone, New Zealand: soft-linked segmentation of a continental rift system. New Zealand Journal of Geology and Geophysics 44, 271–283.

Stagpoole, V.M., Bibby, H.M., 1999. Residual gravity anomaly map of the Taupo Volcanic Zone, New Zealand, 1:250 000. Institute of Geological & Nuclear Sciences, Lower Hutt, New Zealand. Geophysical Map 13.

Taylor, S.K., Bull, J.M., Lamarche, G., Barnes, P.M., 2004. Normal fault growth and linkage in the Whakatane Graben, New Zealand, during the last 1.3 Myr. Journal of Geophysical Research 109 (B2), doi:10.1029/2003JB002412. B02408.

Van Dissen, R.J., Berryman, K.R., 1996. Surface rupture earthquakes over the last ~1000 years in the Wellington region, New Zealand, and implications for ground shaking hazard. Journal of Geophysical Research 101 (B3), 5999–6019.

Villamor, P., Berryman, K.R., 2001. A Late Pleistocene extension rate in the Taupo Volcanic Zone, New Zealand, derived from fault slip data. New Zealand Journal of Geology and Geophysics 44, 243–269.

Villamor, P., Berryman, K.R., 2006. Evolution of the southern termination of the Taupo Rift, New Zealand. New Zealand Journal of Geology & Geophysics 49, 23–37.

Wallace, L.M., Beavan, J., McCaffrey, R., Darby, D., 2004. Subduction zone coupling and tectonic block rotations in the North Island, New Zealand. Journal of Geophysical Research 109 (B12), 2406, doi:10.1029/2004JB003241.

Walsh, J.J., Watterson, J., 1991. Geometric and kinematic coherence and scale effects in normal fault systems. In: Roberts, A.M., Yielding, G., Freeman, B. (Eds.), The Geometry of Normal Faults. Geological Society of London Special Publication, 56, pp. 193–203.

Wilson, C.J.N., Houghton, B.F., McWilliams, M.O., Lamphere, M.A., Weaver, S.D., Briggs, R.M., 1995. Volcanic and structural evolution of Taupo Volcanic Zone, New Zealand: a review. Journal of Volcanology and Geothermal Research 68, 1–28.

Woodward, D.J., 1988. Seismic reflection survey on the Rangitaiki Plains, eastern Bay of Plenty. Department of Scientific and Industrial Research, New Zealand. Geophysics Division research report 218.

Woodward, D.J., 1989. Geological structure of the Rangitaiki Plains near Edgecumbe, New Zealand, from seismic data. New Zealand Journal of Geology and Geophysics 32, 15–16.

Woodward-Clyde, 1998. Matahina Dam strengthening project. Geological Completion Report to Electricity Corporation of New Zealand.

York, D., 1973. Evolution of triple junctions. Nature 244, 341–342.